

Polymeric Organosilicon Systems. 30. Preparation and Properties of Polymers Containing Iron(0)-Complex-Coordinated Silole Units

Joji Ohshita, Takeshi Hamaguchi, Eiji Toyoda, Atsutaka Kunai,*
Kenji Komaguchi, and Masaru Shiotani

Department of Applied Chemistry, Faculty of Engineering, Hiroshima University,
Higashi-Hiroshima 739-8527, Japan

Mitsuo Ishikawa* and Akinobu Naka

Department of Chemical Technology, Kurashiki University of Science and the Arts,
2640 Nishinoura, Tsurashima, Kurashiki, Okayama 712-8505, Japan

Received July 13, 1998

UV irradiation of poly[(tetraethylidisilanylene)(3,4-diethynylsilole)] in the presence of an excess of $\text{Fe}(\text{CO})_5$ led to the formation of $\text{Fe}(\text{CO})_3$ -coordinated silole units in the polymer backbone. The ratio of the $\text{Fe}(\text{CO})_3$ -coordinated and noncoordinated units in the resulting polymer was determined to be 2:1 by ^1H NMR spectrometry. Similar treatment of poly[(tetramethylidisilanylene)(3,4-diethynylsilole)] also afforded the corresponding $\text{Fe}(\text{CO})_3$ -coordinated polymer. The polymers with $\text{Fe}(\text{CO})_3$ -coordinated silole units exhibit slightly red-shifted UV absorption bands, relative to the parent noncoordinated polymers. When doped with FeCl_3 vapor, the $\text{Fe}(\text{CO})_3$ -coordinated polymers became semiconducting with conductivities on the order of 10^{-5} S/cm, much higher than the conductivities of the parent polymers doped with FeCl_3 , which were determined to be less than 10^{-8} S/cm. Crystal structures of two model compounds having $\text{Fe}(\text{CO})_3$ -coordinated or noncoordinated 3,4-diethynylsilole units were determined by X-ray crystallography, which suggest enhanced π -conjugation in the $\text{Fe}(\text{CO})_3$ -coordinated 3,4-diethynylsilole ring as compared with the noncoordinated one.

Introduction

Current interest has been focused on the chemistry of the silole ring system, which shows unique optical properties. The characteristic red-shifted UV absorptions of silole derivatives originate from their low-lying LUMO that is due to the $\sigma^*-\pi^*$ interaction between the silole silicon atom and the π -orbitals.¹ Highly electron transporting properties of cooligomers of silole-2,5-diyl and heteroaromatic systems² and dithienosiloles having a silole ring fused with two thiophene rings³ also reflect the low-lying LUMO of the silole ring systems.

Introduction of silole units into conjugated polymers has been also studied extensively, and polymers with silole-1,1-diyl,⁴ silole-2,5-diyl,^{5,6} and dithienosilole-2,6-

diyl units⁷ have been reported so far. Of these, Tamao et al. have recently demonstrated that polymers with alternating silole-2,5-diyl and oligothiophene units exhibit highly conducting properties in their doped states.⁵

In the course of our studies concerning the synthesis and properties of polymers with alternating organosilicon and π -conjugated carbon units,⁸ we have demonstrated that anionic ring-opening polymerization (ROP) of 4,5,10-trisilabicyclo[6.3.0]undeca-1(11),8-diene-2,6-diyne (**1**) in the presence of a catalytic amount of tetrabutylammonium fluoride (TBAF) affords poly[disilanylene(3,4-diethynylsiloles)] (**2**) with high molecular weights in high yields, as shown in Scheme 1.⁹ Polymers **2**, however, exhibit blue-shifted UV absorptions relative to those of poly[disilanylene(2,5-diethynylsiloles)] (**2'**) prepared by palladium-catalyzed dehydrobromination of 2,5-dibromotetraphenylsilole and 1,2-diethynylsilanes (Chart 1).¹⁰ This is probably due to the interruption of π -conjugation between carbons at 3,4-positions in the silole ring for polymers **2**.

(1) (a) Yamaguchi, S.; Tamao, K. *Bull. Chem. Soc. Jpn.* **1996**, *69*, 2327. (b) Yamaguchi, S. *Synth. Met.* **1996**, *82*, 149. (c) Hong, S. Y.; Song, J. M. *Chem. Mater.* **1997**, *9*, 297.

(2) (a) Tamao, K.; Ohno, S.; Yamaguchi, S. *Chem. Commun.* **1996**, 1873. (b) Tamao, K.; Uchida, M.; Izumikawa, T.; Furukawa, K.; Yamaguchi, S. *J. Am. Chem. Soc.* **1996**, *118*, 11974.

(3) Adachi, A.; Ohshita, J.; Kunai, A.; Okita, K.; Kido, J. *Chem. Lett.* **1998**, 1233.

(4) (a) Albizane, A.; Corriu, R. J. P.; Douglas, W. E.; Fisch, H. *Polym. Int.* **1993**, *26*, 93. (b) Corriu, R. J. P.; Douglas, W. E.; Yang, Z.-X. *J. Organomet. Chem.* **1993**, *456*, 35.

(5) (a) Tamao, K.; Yamaguchi, S.; Shiozaki, M.; Nakagawa, Y.; Ito, Y. *J. Am. Chem. Soc.* **1992**, *114*, 5867. (b) Tamao, K.; Yamaguchi, S.; Ito, Y.; Matsuzaki, Y.; Yamabe, T.; Fukushima, M.; Mori, S. *Macromolecules* **1995**, *28*, 8668.

(6) Yamaguchi, S.; Iimura, K.; Tamao, K. *Chem. Lett.* **1998**, 89.

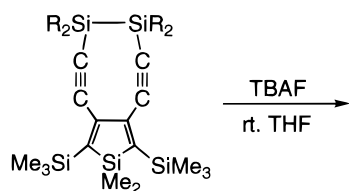
(7) Ohshita, J.; Nodono, M.; Watanabe, T.; Ueno, Y.; Kunai, A.; Harima, Y.; Yamashita, K.; Ishikawa, M. *J. Organomet. Chem.* **1998**, *553*, 487.

(8) Ohshita, J.; Kunai, A. *Acta Polym.* **1998**, *49*, 379.

(9) Toyoda, E.; Kunai, A.; Ishikawa, M. *Organometallics* **1995**, *14*, 1089.

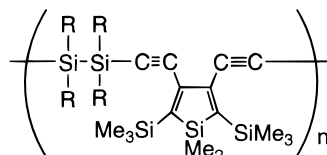
(10) Ohshita, J.; Mimura, N.; Nodono, M.; Kunai, A.; Komaguchi, K.; Shiotani, M.; Ishikawa, M. *Macromolecules* **1998**, *31*, 7985.

Scheme 1



1a R = Et

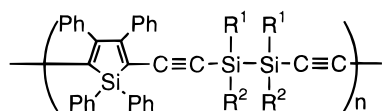
1b R = Me



2a R = Et

2b R = Me

Chart 1

2' R¹ = Ph, R² = MeR¹ = Hex, R² = MeR¹ = R² = Me

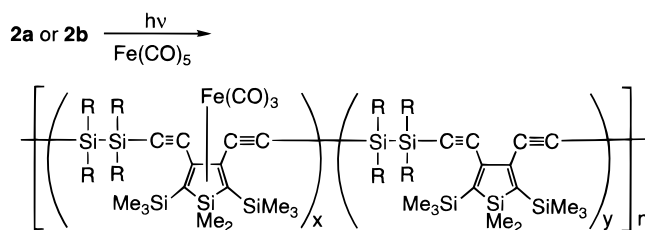
It is of interest to us to investigate the incorporation of metal coordination into the silole ring of the polymers, which would provide new opportunities to modify the properties of the polymers. Corriu et al. have previously reported the formation of polymers having iron carbonyl coordinated silole-1,1-diyl units.^{4b} However, no studies concerning the complexation of silole polymers with the other mode of substitution have been reported so far. In this paper, we report complexation of iron carbonyl to the silole rings in poly[disilanylene(3,4-diethynylsiloles)]. We also describe the properties of the resulting polymers, including enhanced conducting properties of the polymers relative to the parent species.

Results and Discussion

Preparation of Fe-Coordinated Polymers. Irradiation of a benzene solution of polymer **2a** with a high-pressure mercury lamp in the presence of 5 equiv of Fe(CO)₅ afforded polymer **3a** in 88% yield (Scheme 2). Monitoring the reaction progress by ¹H NMR spectrometry of the reaction mixture showed that the signals due to the starting polymer decreased gradually and new signals assignable to Fe(CO)₃-coordinated silole units appeared and increased with an increase in the irradiation period. After 4 h of irradiation, the ratio of the Fe(CO)₃-coordinated silole units (*x*) and the starting noncoordinated units (*y*) reached a maximum value of *x*/*y* = 2/1. Prolonged irradiation, however, led to the formation of a large amount of insoluble materials and a decrease of the ratio *x*/*y*. After 10 h of irradiation, only a 20% yield of the soluble polymer with *x*/*y* = 1/2 was obtained.

The structure of polymer **3a** was confirmed mainly by NMR spectrometric analysis. Its ¹H NMR spectrum

Scheme 2



3a R = Et

3b R = Me

shows broad signals due to nonequivalent methyl groups on the silole silicon atom at -0.19 and 0.58 ppm, in addition to signals due to trimethylsilyl and ethyl protons and those for the starting Fe-free units. The ¹³C and ²⁹Si NMR spectra of polymer **3a** are also consistent with the proposed structure shown in Scheme 2 and reveal signals ascribed to both Fe-coordinated and noncoordinated units. Each of the sp and sp² carbons, and silole and disilane silicons, however, splits into two or three signals. These splittings may be explained in terms of random incorporation of Fe-coordinated units in the polymer backbone. The ¹³C NMR spectrum shows signals around 56 and 96 ppm characteristic of metal-coordinated butadiene units.¹¹ In contrast, the signals of sp carbons of Fe-coordinated diethynylsilole units are at about 98 and 106 ppm, which are only slightly shifted from those of the starting diethynylsilole units, indicating that no significant interaction takes place between the ethynylene units and the Fe-complex center. The IR spectrum shows absorptions due to carbonyl stretching frequencies at 1983 and 2045 cm⁻¹. A stretching band of the ethynylene bond appears at 2132 cm⁻¹, at essentially the same energy as that of polymer **2a** (2130 cm⁻¹), in agreement with the absence of a significant interaction with the Fe-complex center. The IR spectrum of polymer **2a** reveals a strong absorption band at 1454 cm⁻¹, probably due to the stretching frequencies of silole C=C bonds. In the spectrum of **3a**, however, only a weak band is observed in this region, again indicating the coordination of the Fe-complex center with the silole ring.

Similar photolysis of polymer **2b** in the presence of Fe(CO)₅ afforded polymer **3b**. Polymer **3b**, however, is hardly soluble in organic solvents, and therefore, ¹³C and ²⁹Si NMR spectroscopic analysis of **3b** could not be carried out. Its ¹H NMR spectrum shows a broad singlet at 0.13 ppm due to the trimethylsilyl protons of Fe-coordinated units. The other signals, however, are not observed due to the low solubility of polymer **3b**. The IR spectrum of **3b** reveals stretching bands at 1985 and 2045 cm⁻¹ and at 2149 cm⁻¹, due to the stretching frequencies of C=O and C≡C bonds, respectively.

Some properties of polymers **3a,b** are summarized in Table 1, in comparison with those of **2a,b**. Molecular weights of the polymers were determined by GPC relative to polystyrene standards to be *M*_w = 11 400 (*M*_w/*M*_n = 4.3) for **3a** and *M*_w = 5500 (*M*_w/*M*_n = 4.5) for **3b**, which are smaller than the calculated values based on the molecular weights of the starting polymers **2a** (*M*_w

(11) Mann, B. E.; Taylor, B. F. *¹³C NMR Data for Organometallic Compounds*; Academic Press: London, 1981.

Table 1. Properties of Polymers 2a,b and 3a,b

polymer	UV ^a λ_{\max} /nm	conductivity/ (S/cm) ^b	TGA ^c	
			$T_d^{5\%}$ /°C ^d	wt loss/% ^e
2a	210, 255, 300 (sh)	$<10^{-8}$	309	76
3a	209, 249 (sh), 324 (sh)	3.3×10^{-5} (1.4×10^{-5})	171	61
2b	254, 292 (sh)	$<10^{-8}$	290	67
3b	209, 323 (sh)	5.0×10^{-5}	190	70

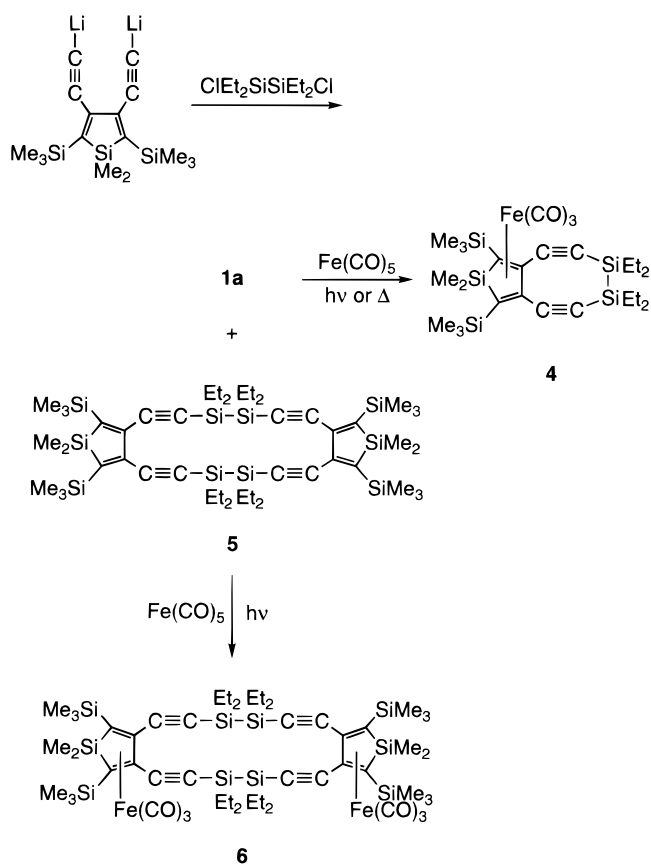
^a In THF. ^b On a polymer film, determined by the four-probe method; doped with FeCl₃ (I₂). ^c Under a nitrogen atmosphere with a rate of 20 °C/min. ^d Temperature of 5% weight loss. ^e Total weight loss at 1000 °C based on the initial weight.

= 41 800, $M_w/M_n = 1.5$) and **2b** ($M_w = 12\ 700$, $M_w/M_n = 3.1$). This seems to be due to the cleavage of Si–Si bonds in the polymer main chain during the photolysis, as observed for the other polymers with alternating disilanylene and π -conjugated carbon units.⁸ The UV spectra of polymers **3a,b** reveal a strong peak at 209 nm bearing weaker broad shoulders, which are at longer wavelengths than those observed for polymers **2a,b**. Furthermore, the absorption edges of **3a,b** are around 420 nm, which are also red-shifted as compared with those of **2a,b** (ca. 380 nm), indicating narrower band gaps for **3a,b**.

Polymers **3a,b** are insulators but became conducting upon doping of the polymer films with FeCl₃ or I₂ vapor in vacuo. The conductivities increased with an increase in the doping period and reached to maximum values on the order of 10^{-5} S/cm as listed in Table 1, in marked contrast to polymers **2a,b**, whose doping with FeCl₃ or I₂ under the same conditions no longer gave conducting films ($<10^{-8}$ S/cm). Narrower band gaps of polymers **3a,b** suggested by UV spectrometry seem to be the reason for the higher conductivities of doped polymers **3a,b** compared to those of **2a,b**. When an I₂-doped film of polymer **3a** was dedoped under reduced pressure, the polymer changed again to an insulator. The IR spectrum of the resulting dedoped polymer **3a** shows a decrease in the absorption bands due to the stretching frequencies of the carbonyl ligands. The intensities of the CO stretching bands are approximately one-third of the initial values of the starting polymer **3a**. In addition, the absorption at about 1460 cm⁻¹, characteristic of the noncoordinated diethynylsilole system, increased. The dedoped polymer could be doped again with I₂ vapor with a maximum conductivity of 5.6×10^{-6} S/cm, slightly lower than that obtained from the first doping experiment. These results clearly indicate that polymer **3a** is fairly stable upon doping with I₂ vapor and dedoping under reduced pressure but underwent liberation of Fe(CO)₃ units to produce coordination-free diethynylsilole units in part.

Thermal properties of the polymers were examined by thermogravimetric analysis (TGA) under a nitrogen atmosphere, and the results are also summarized in Table 1. As indicated by the lower temperatures of 5% weight loss ($T_d^{5\%}$), polymers **3a,b** decomposed at lower temperatures than **2a,b**, probably due to the liberation of iron carbonyls from polymers **3a,b**.

Preparation of Model Compounds. To learn how the coordination of the Fe complex affects the structure of the silole ring system, we synthesized model compounds and examined them with respect to their IR and UV spectra. Thus, irradiation of a benzene solution of

Scheme 3**Table 2. Properties of Compounds 1a and 4–6**

compd	UV ^a	
	λ_{\max} /nm	λ_{edge} /nm
1a	227, 250, 340 (sh) ^b	380
4	220, 244, 344 (sh) ^b	420
5	210, 268, 301	390
6	210, 237, 320	430

^a In THF. ^b Shoulder.

compound **1a** in the presence of an excess of Fe(CO)₅ afforded Fe(CO)₃-coordinated silole **4** in 15% yield (Scheme 3). A higher yield of **4** was achieved by heating **1a** with Fe(CO)₅ at 150 °C in an autoclave (87% yield). The low yield of **4** from the photolysis may be due to the decomposition of **1a** under the reaction conditions. Similar photolysis of **5** which has a dimeric structure of **1a** and was obtained as a byproduct in the synthesis of **1a**, afforded the Fe–silole complex **6** as a 1:1 mixture of cis and trans isomers in 54% yield.

The structures of Fe complexes **4** and **6** were confirmed by spectrometry and elemental analysis. The chemical shifts for the signals of the Fe(CO)₃-coordinated 3,4-diethynylsilole ring in the ¹H, ¹³C, and ²⁹Si NMR spectra closely resemble those of polymer **3a**. The UV absorption maxima and edges of **4** and **6** (Table 2) are red-shifted from those of **1a** and **5**, as observed for polymers **3a,b**.

To obtain a polymer whose silole units are fully coordinated with the Fe complex, we examined the ROP of compound **4**. However, all attempts to polymerize **4** under several conditions, such as heating at 80 °C in the presence of a catalytic amount of TBAF, were unsuccessful, in contrast to the case for **1a**, whose

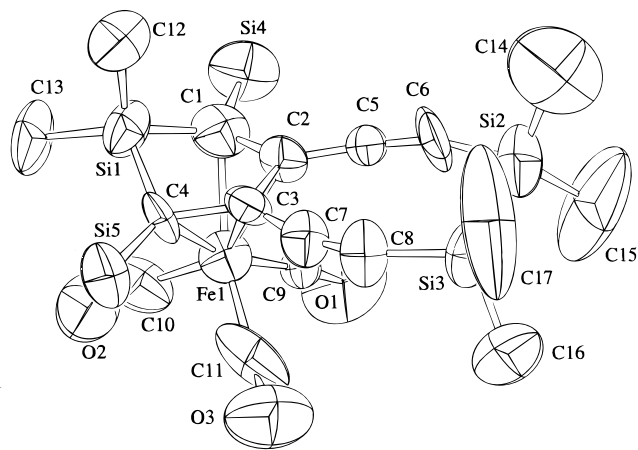


Figure 1. ORTEP drawing of compound **4** with the atomic numbering scheme. Methyl carbons of trimethylsilyl and ethyl groups are omitted for clarity. Thermal ellipsoids are drawn at 50% probability.

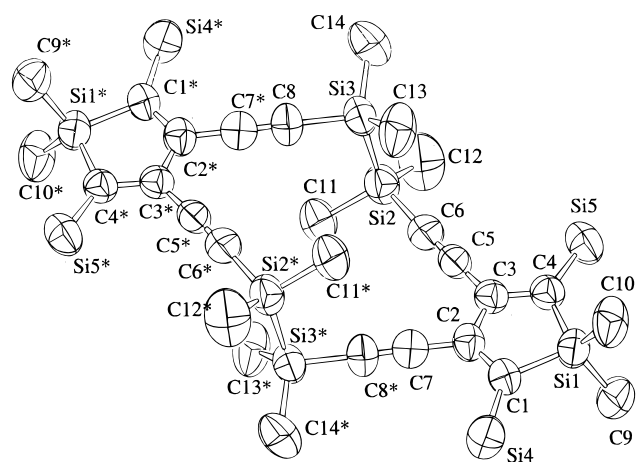


Figure 2. ORTEP drawing of compound **5** with the atomic numbering scheme. Methyl carbons of trimethylsilyl and ethyl groups are omitted for clarity. Thermal ellipsoids are drawn at 50% probability.

TBAF-catalyzed ROP takes place at room temperature (see Scheme 1).⁹

Crystal Structures of 4 and 5. Crystal structures of compounds **4** and **5** were determined by X-ray diffraction studies. ORTEP drawings of them are depicted in Figures 1 and 2. Cell dimensions, data collection and refinement parameters, and selected bond distances and angles are given in Tables 3–5.

When the silole ring structures in **4** and **5** are compared, the $C(\beta)$ – $C(\beta')$ length in **4** (1.41 Å) is shorter than that in **5** (1.50 Å), while the $C(\alpha)$ – $C(\beta)$ length is found to be longer in **4** (1.49 Å in average) than in **5** (1.39 Å in average). These results clearly indicate that the Fe coordination to the silole ring leads to an increase in the bond order of $C(\beta)$ – $C(\beta')$ and a decrease in that of $C(\alpha)$ – $C(\beta)$. The Si– $C(\alpha)$ length is little affected by the Fe coordination.

Since no crystal structures of **1** have been obtained due to the rapid decomposition of the crystals of **1** upon exposure to X-ray radiation, it is not known how the coordination of the Fe complex affects the crystal structure of **4**. However, when we compare the structure of the eight-membered ring of **4** with those of *cis*, *trans*- and *all-trans*-1,2,5,6-tetramethyl-1,2,5,6-tetraphenyl-

Table 3. Crystal Data, Experimental Conditions, and Summary of Structural Refinement for **4** and **5**

	4	5
mol formula	C ₂₇ H ₄₄ Si ₅ FeO ₃	C ₄₈ H ₈₈ Si ₁₀
mol wt	910.18	946.08
space group	<i>P</i> 2 ₁ / <i>n</i>	<i>P</i> 2 ₁ / <i>c</i>
cell dimens		
<i>a</i> , Å	12.68(1)	12.482(4)
<i>b</i> , Å	22.22(1)	14.208(4)
<i>c</i> , Å	14.119(6)	18.665(3)
β , deg	115.54(4)	101.64(2)
<i>V</i> , Å ³	3589(3)	3242(1)
<i>Z</i>	2	2
<i>D</i> _{calcd} , Mg/m ³	0.834	0.969
<i>F</i> ₀₀₀	940.00	1032.00
cryst size, mm ³	0.6 × 0.4 × 0.1	0.6 × 0.5 × 0.2
cryst color	yellow	colorless
μ , mm ⁻¹	2.69	2.1026
diffractometer	Rigaku AFC-6C	Rigaku AFC-6C
temp, K	298	298
wavelength, Å	1.5418 (Cu K α)	1.5418 (Cu K α)
monochromator	graphite cryst	graphite cryst
scan type	ω -2 θ	ω -2 θ
scan speed, deg/min	4	4
scan width, deg	0 < 2 θ < 125.7	0 < 2 θ < 126.1
diffraction geom	sym A	sym A
<i>hkl</i> range		
<i>h</i>	0 ≤ <i>h</i> ≤ 15	0 ≤ <i>h</i> ≤ 14
<i>k</i>	0 ≤ <i>k</i> ≤ 26	0 ≤ <i>k</i> ≤ 16
<i>l</i>	-16 ≤ <i>l</i> ≤ 16	-21 ≤ <i>l</i> ≤ 21
no. of unique rflns	4226	5103
no. of obsd rflns (<i>I</i> > 3 σ (<i>I</i>))	1029	2768
<i>R</i>	0.059	0.082
<i>R</i> _w ^a	0.063	0.084

^a Weighting scheme is $(\sigma(F_o))^2 + 0.0004|F_o|^2$.

Table 4. Selected Distances (Å) and Angles (deg) for Compound **4** with Their Esd's in Parentheses

Fe(1)–C(1)	2.16(2)	Fe(1)–C(2)	2.10(2)	Fe(1)–C(3)	2.04(2)
Fe(1)–C(4)	2.18(2)	Fe(1)–C(9)	1.77(3)	Fe(1)–C(10)	1.77(3)
Fe(1)–C(11)	1.83(4)	Si(1)–C(1)	1.85(3)	Si(1)–C(4)	1.87(2)
Si(1)–C(12)	1.83(2)	Si(1)–C(13)	1.84(2)	Si(2)–Si(3)	2.39(1)
Si(2)–C(6)	1.84(3)	Si(2)–C(14)	1.84(6)	Si(2)–C(15)	1.86(4)
Si(3)–C(8)	1.84(3)	Si(3)–C(16)	1.86(4)	Si(3)–C(17)	1.84(4)
Si(4)–C(1)	1.89(3)	Si(5)–C(4)	1.85(2)	O(1)–C(9)	1.14(2)
O(2)–C(10)	1.16(2)	O(3)–C(11)	1.11(3)	C(1)–C(2)	1.49(3)
C(2)–C(3)	1.41(3)	C(2)–C(5)	1.49(3)	C(3)–C(4)	1.48(3)
C(3)–C(7)	1.50(3)	C(5)–C(6)	1.17(3)	C(7)–C(8)	1.19(3)
C(14)–C(18)	1.17(5)	C(15)–C(19)	1.35(6)	C(16)–C(20)	1.28(5)
C(17)–C(21)	1.14(5)				
C(1)–Si(1)–C(4)	89(1)	C(1)–Si(1)–C(12)	112(1)		
C(1)–Si(1)–C(13)	116(1)	C(4)–Si(1)–C(12)	113(1)		
C(4)–Si(1)–C(13)	116(1)	C(12)–Si(1)–C(13)	107(1)		
Si(3)–Si(2)–C(6)	104.1(9)	Si(3)–Si(2)–C(14)	111(2)		
Si(3)–Si(2)–C(15)	112(1)	C(6)–Si(2)–C(14)	109(1)		
C(6)–Si(2)–C(15)	105(2)	C(14)–Si(2)–C(15)	111(3)		
Si(2)–Si(3)–C(8)	101.5(9)	Si(2)–Si(3)–C(16)	111(1)		
Si(2)–Si(3)–C(17)	112(2)	C(8)–Si(3)–C(16)	106(1)		
C(8)–Si(3)–C(17)	110(1)	Si(1)–C(1)–Si(4)	126(1)		
Si(1)–C(1)–C(2)	106(1)	Si(4)–C(1)–C(2)	121(1)		
C(1)–C(2)–C(3)	108(2)	C(1)–C(2)–C(5)	132(2)		
C(3)–C(2)–C(5)	118(2)	C(2)–C(3)–C(4)	119(2)		
C(2)–C(3)–C(7)	115(2)	C(4)–C(3)–C(7)	125(2)		
Si(1)–C(4)–Si(5)	128(1)	Si(1)–C(4)–C(3)	101(1)		
Si(5)–C(4)–C(3)	124(1)	C(2)–C(5)–C(6)	168(2)		
Si(2)–C(6)–C(5)	152(2)	C(3)–C(7)–C(8)	161(2)		
Si(3)–C(8)–C(7)	157(2)	Fe(1)–C(9)–O(1)	172(2)		
Fe(1)–C(10)–O(2)	174(2)	Fe(1)–C(11)–O(3)	174(3)		

1,2,5,6-tetrasilacyclooctadiynes **7** reported previously (Figure 3),¹² there appear to be no obvious differences in the bond lengths and angles, except for the narrowing of the Si–C≡C angle in compound **4**. This is in contrast to the fact that **4** did not undergo anionic ROP while

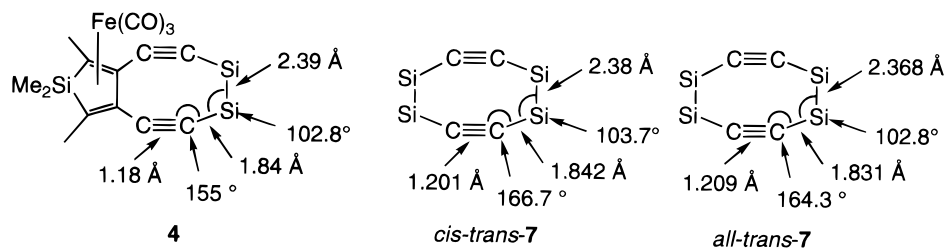


Figure 3. Bond lengths and angles for compounds **4** and *cis-trans*- and *all-trans*-**7**. Values given are averages.

Table 5. Selected Distances (Å) and Angles (deg) for Compound **5 with Their Esd's in Parentheses**

Si(1)–C(1)	1.884(8)	Si(1)–C(4)	1.874(8)	Si(1)–C(9)	1.849(9)
Si(1)–C(10)	1.892(9)	Si(2)–Si(3)	2.390(4)	Si(2)–C(6)	1.84(1)
Si(2)–C(11)	1.884(9)	Si(2)–C(12)	1.86(1)	Si(3)–C(8)	1.835(9)
Si(3)–C(13)	1.88(1)	Si(3)–C(14)	1.89(1)	Si(4)–C(1)	1.831(8)
Si(5)–C(4)	1.862(8)	C(1)–C(2)	1.39(1)	C(2)–C(3)	1.50(1)
C(2)–C(7)	1.45(1)	C(3)–C(4)	1.39(1)	C(3)–C(5)	1.45(1)
C(5)–C(6)	1.18(1)	C(7)–C(8*)	1.19(1)		
C(1)–Si(1)–C(4)	95.3(4)	C(1)–Si(1)–C(9)	112.1(4)		
C(1)–Si(1)–C(10)	112.5(4)	C(4)–Si(1)–C(9)	112.7(4)		
C(4)–Si(1)–C(10)	112.9(4)	C(9)–Si(1)–C(10)	110.5(4)		
Si(3)–Si(2)–C(6)	105.6(3)	Si(3)–Si(2)–C(11)	109.6(4)		
Si(3)–Si(2)–C(12)	116.2(5)	C(6)–Si(2)–C(11)	107.3(5)		
C(6)–Si(2)–C(12)	106.3(5)	C(11)–Si(2)–C(12)	111.3(6)		
Si(2)–Si(3)–C(8)	105.0(3)	Si(2)–Si(3)–C(13)	109.2(4)		
Si(2)–Si(3)–C(14)	115.2(4)	C(8)–Si(3)–C(13)	108.4(5)		
C(8)–Si(3)–C(14)	106.3(5)	C(13)–Si(3)–C(14)	112.2(6)		
Si(1)–C(1)–Si(4)	130.3(5)	Si(1)–C(1)–C(2)	104.0(6)		
Si(4)–C(1)–C(2)	125.7(6)	C(1)–C(2)–C(3)	118.7(7)		
C(1)–C(2)–C(7)	122.9(8)	C(3)–C(2)–C(7)	118.4(7)		
C(2)–C(3)–C(4)	116.2(7)	C(2)–C(3)–C(5)	119.3(7)		
C(4)–C(3)–C(5)	124.4(8)	Si(1)–C(4)–Si(5)	130.8(5)		
Si(1)–C(4)–C(3)	105.7(6)	Si(5)–C(4)–C(3)	123.4(6)		
C(3)–C(5)–C(6)	178.8(9)	Si(2)–C(6)–C(5)	176.8(8)		
C(2)–C(7)–C(8*)	177.8(9)	Si(3)–C(8)–C(7*)	174.3(8)		

compounds **7** readily polymerize to give the corresponding high polymers by anionic or thermally induced ROP.^{12,13} The reluctance of **4** to undergo ROP, therefore, seems to be due to steric protection by the Fe(CO)₃ group, rather than released ring strain by coordination of the Fe complex.

MO Calculations on Model Compounds. To obtain more information about the electronic states of the Fe(CO)₃-coordinated and noncoordinated 3,4-diethynylsilole system, we performed ab initio molecular orbital (MO) calculations for simplified model compounds **8** and **9**. The geometries of **8** and **9** were optimized by molecular mechanics (MM2), and the STO-3G basis set is employed for the calculations. When we compare the optimized geometries of silole ring systems of compounds **8** and **9**, the C(β)–C(β') bond length is shortened (1.48 Å for **8**, 1.36 Å for **9**) and the C(α)–C(β) length (1.34 Å for **8**, 1.52 Å for **9**) is elongated by Fe(CO)₃ coordination, agreeing with the results of X-ray diffraction studies on compounds **4** and **5**. Figure 4 represents the energy diagram for **8** and **9**, with a smaller HOMO–LUMO energy gap for **9** than for **8**. The difference in HOMO levels (ca. 3.27 eV) for **8** and **9** is much greater than that of the respective LUMOs (ca. 0.36 eV), and hence is primarily responsible for the smaller HOMO–LUMO gap for **9**. The HOMO and LUMO of **8** cor-

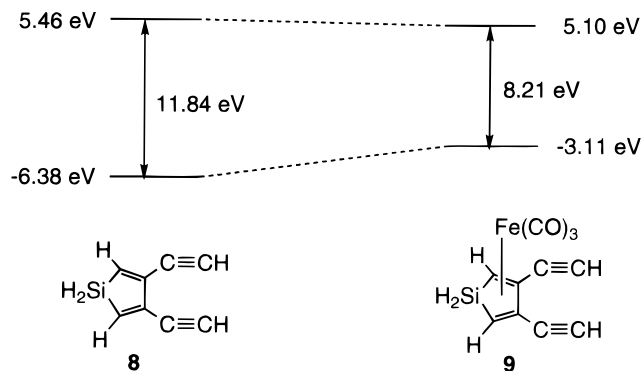


Figure 4. Relative energy levels for the HOMO and LUMO of compounds **8** and **9**, derived from RHF/STO-3G calculations.

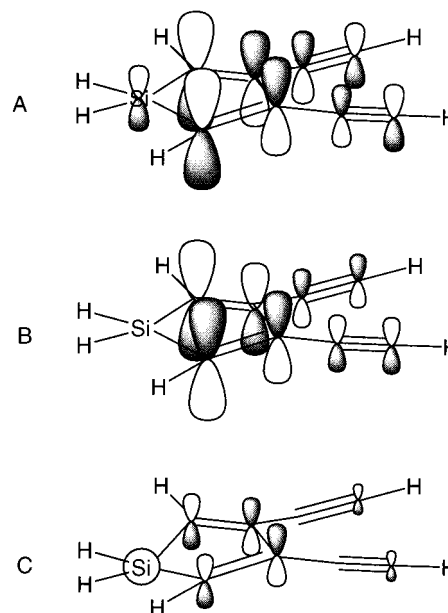


Figure 5. Orbital patterns for the (A) LUMO and (B) HOMO of **8** and (C) HOMO of **9**. A coordinating part of Fe(CO)₃ is omitted for **9**.

respond to π and π^* orbitals, respectively (Figure 5B,A). The LUMO of **9** is localized on almost 4d atomic orbitals of Fe, while its HOMO is contributed to by both 4d atomic orbitals of Fe and 2p atomic orbitals of carbons of the diethynylsilole unit. Interestingly, the orbital pattern of the diethynylsilole fragment of the HOMO of **9** (Figure 5C) closely resembles the LUMO pattern of **8**, indicating the significant influence of Fe(CO)₃ coordination on the electronic state of the diethynylsilole system.

Conclusions

We have synthesized Fe-coordinated poly[(disilanylene)(3,4-diethynylsiloles)] by the photolysis of poly-

(12) Ishikawa, M.; Hatano, T.; Hasegawa, Y.; Horio, T.; Kunai, A.; Miyai, A.; Ishida, T.; Tsukihara, T.; Yamanaka, T.; Koike, T.; Shioya, J. *Organometallics* **1992**, *11*, 1604.

(13) Ishikawa, M.; Horio, T.; Hatano, T.; Kunai, A. *Organometallics* **1993**, *12*, 2078.

[(disilanylene)(3,4-diethynylsiloles)] in the presence of an excess of $\text{Fe}(\text{CO})_5$. UV spectrometric analysis of the Fe-coordinated polymers indicates narrower band gaps for the Fe-coordinated ones, as compared with the noncoordinated ones. Reflecting this, the Fe-coordinated polymers exhibited higher conducting properties upon doping with FeCl_3 vapor, relative to the parent noncoordinated polymers.

MO calculations on model compounds suggest that elevating of the HOMO energy level by coordination with $\text{Fe}(\text{CO})_3$ is mainly responsible for the narrower band gap. It is also likely that the increase of the bond order of $\text{C}(\beta)\text{--C}(\beta')$, indicated by both MO calculations and X-ray diffraction studies of compounds **4** and **5**, permits conjugation between ethynyl groups through this bond to enhance the π -conjugation in the diethynylsilole system. This may be also responsible for the increase of conductivities of doped polymers by Fe coordination.

Experimental Section

General Considerations. All reactions were carried out under an atmosphere of dry nitrogen. ^1H , ^{13}C , and ^{29}Si NMR spectra were recorded on JEOL Model JNM-EX 270 and JEOL Model JNM-LA 400 spectrometers. EI mass spectra were measured with Shimadzu GCMS QP-1000 and Hitachi M-80B spectrometers. FAB mass spectra were measured on a JEOL Model JMS-700 spectrometer. UV spectra were measured on a Hitachi U-3210 spectrophotometer, and IR spectra were measured on a Perkin-Elmer FT-IR Model 1600 spectrometer. Molecular weights of the polymers were determined by gel-permeation chromatography relative to polystyrene standards, using Shodex 806 and 804 as the column and THF as the eluent.

Materials. THF and benzene were dried over sodium-potassium alloy and lithium aluminum hydride, respectively, and distilled just before use.

Preparation of 1,1-Dimethyl-2,5-bis(trimethylsilyl)-3,4-diethynylsilole. A mixture of 10.02 g (51.52 mmol) of bis(trimethylsilyl)butadiyne, 3.30 g (27.89 mmol) of 1,1,2,2-tetramethyldisilane, and 0.60 g (1.64 mmol) of dichlorobis(triethylphosphine)nickel(II) in 50 mL of dry THF was heated to reflux for 26 h. The reaction mixture was concentrated and passed through a short column to remove nonvolatile substances. Recrystallization from methanol gave a mixture of 1,1-dimethyl-2,5-bis(trimethylsilyl)-3,4-bis(trimethylsilyl)ethynylsilole and 1,1,4,4-tetramethyl-2,5-bis(trimethylsilyl)-3,6-bis(trimethylsilyl)ethynyl-1,4-disilacyclohexa-2,5-diene in 38% combined yield. The mixture was treated with ca. 50 mL of methanol in the presence of a catalytic amount of potassium hydroxide (30 mg) at 50 °C for 1 h. The resulting mixture was concentrated and chromatographed on silica gel using hexane as the eluent to give 2.09 g (27% yield) of the title compound, together with 1.02 g (11% yield) of 1,1,4,4-tetramethyl-2,5-bis(trimethylsilyl)-3,6-diethynyl-1,4-disilacyclohexa-2,5-diene. Data for these compounds have been already reported.⁹

Preparation of 1a and 5. To a solution of 2.05 g (6.79 mmol) of 1,1-dimethyl-2,5-bis(trimethylsilyl)-3,4-diethynylsilole in 150 mL of dry THF was added a THF solution of 13.8 mmol of lithium diisopropylamide prepared from diisopropylamine and an equimolar amount of *n*-butyllithium/hexane (1.54 M) in 10 mL of THF at -80 °C. The mixture was stirred at -80 °C for 0.5 h. To this was added a solution of 1.65 g (6.79 mmol) of 1,2-dichlorotetraethyldisilane in 30 mL of THF at -80 °C over a period of 1 h. The mixture was stirred at -80 °C for 1 h and then warmed to 0 °C. The resulting mixture was hydrolyzed with 150 mL of dilute aqueous hydrochloric acid. The organic layer was separated, and the aqueous layer

was extracted with ether. The organic layer and the extracts were combined, washed with water, and dried over anhydrous magnesium sulfate. After evaporation of the solvent, the residue was passed through a silica gel short column using hexane as the eluent. Recrystallization from ethanol gave 1.72 g (54% yield) of **1a** as colorless crystals. Compound **5** was obtained as a fraction from column chromatography in 5% yield and recrystallized from ethanol for further reactions. Data for **1a** have been already reported.⁹ Data for **5**: colorless crystals; mp 227–229 °C; FAB MS m/z 945 (M^+); UV (in THF; λ_{max} , nm (ϵ , $M^{-1}\text{cm}^{-1}$)) 210 ($\epsilon = 37\,800$), 268 ($\epsilon = 45\,000$), 301 ($\epsilon = 27\,300$); IR (cm^{-1}) $\nu_{\text{C}=\text{C}}$ 2139; ^1H NMR (δ in CDCl_3) 0.19 (s, 36H, Me_3Si), 0.23 (s, 12H, Me_2Si), 0.83–1.10 (m, 40H, EtSi); ^{13}C NMR (δ in CDCl_3) -3.60 (Me_2Si), -0.79 (Me_3Si), 4.85, 8.24 (EtSi), 97.78, 107.34 (C=C), 146.00, 154.34 (C=C); ^{29}Si NMR (δ in CDCl_3) -30.79, -8.80, 24.18. Anal. Calcd for $\text{C}_{48}\text{H}_{88}\text{Si}_{10}$: C, 60.94; H, 9.38. Found: C, 60.84; H, 9.34.

Compound **1b** was prepared as described for **1a**. Data for **1b** have been previously reported.⁹

Preparation of Polymer 2a. A mixture of 195 mg (0.412 mmol) of **1a** and 0.008 mmol (2 mol %) of tetrabutylammonium fluoride in 1 mL of THF was stirred in a sealed tube at room temperature for 24 h. After addition of a few drops of MeI, the mixture was poured into ca. 50 mL of methanol. The resulting solid was filtered off and dried under reduced pressure to give 169 mg (87% yield) of polymer **2a**.

Polymer **2b** was prepared as described for **2a**. Data for **2a** and **2b** have been previously reported.⁹

Preparation of Polymer 3a. A mixture of 100 mg (0.212 mmol) of polymer **2a** ($M_w = 41\,800$, $M_w/M_n = 1.5$) and 210 mg (1.02 mmol) of $\text{Fe}(\text{CO})_5$ in 80 mL of benzene was irradiated with a high-pressure mercury lamp equipped with a Pyrex filter for 4 h. After evaporation of the solvent, the resulting polymer was dissolved in hexane. The hexane-insoluble part was filtered off, and the filtrate was evaporated; then the residue was reprecipitated from benzene-methanol to give 105 mg (88% yield) of polymer **3a** as brown solids: $M_w = 11\,400$ ($M_w/M_n = 4.3$); UV (in THF; λ_{max} , nm (ϵ , $M^{-1}\text{cm}^{-1}$)) 209 ($\epsilon = 24\,200$), 249 (sh, $\epsilon = 6600$), 324 (sh, $\epsilon = 2500$); IR (cm^{-1}) $\nu_{\text{C}=\text{O}}$ 1983, 2045, $\nu_{\text{C}=\text{C}}$ 2132; ^1H NMR (δ in CDCl_3); signals denoted -Fe are those of Fe-coordinated units) -0.19 (s, 2H, *exo*-MeSi-Fe), 0.01 (s, 2H, Me_2Si), 0.06 (br s, 12H, $\text{Me}_3\text{Si-Fe}$), 0.14 (s, 6H, Me_3Si), 0.58 (s, 2H, *endo*-MeSi-Fe), 0.91, 1.13 (2 br. s, 20H, EtSi-Fe and EtSi); ^{13}C NMR (δ in C_6D_6) -3.73 (Me_2Si), -0.32 (Me_3Si), 1.13 (*exo*-MeSi-Fe), 1.34 ($\text{Me}_3\text{Si-Fe}$), 5.47 (EtSi-Fe), 5.56 (EtSi), 8.99 (EtSi-Fe and *endo*-MeSi), 9.06 (EtSi), 56.32, 95.75, 96.22 (C=C-Fe), 97.65, 97.72 (C=C-Fe), 97.89, 97.94 (C=C), 105.96, 106.11 (C=C-Fe), 108.23, 108.51 (C=C), 146.76, 155.54, 155.57 (C=C), 210.08 (CO-Fe), overlapping of the signals of EtSi-Fe and *endo*-MeSi was indicated by the C-H COSY spectrum; ^{29}Si NMR (δ in C_6D_6) -29.94, -29.92, -29.31 (disilane), -0.65 (Me_3Si), 24.53, 24.57 (silole-Fe), 27.44, 27.56, 27.67 (silole). Anal. Found: C, 42.70; H, 6.70.

Polymer **3b** was prepared from polymer **2b** ($M_w = 12\,700$; $M_w/M_n = 3.1$) as described for **3a**. Data for **3b**: brown solids; $M_w = 5500$ ($M_w/M_n = 4.5$); UV (in THF; λ_{max} , nm (ϵ , $M^{-1}\text{cm}^{-1}$)) 209 ($\epsilon = 9000$), 323 (sh, $\epsilon = 1900$); IR (cm^{-1}) $\nu_{\text{C}=\text{O}}$ 1985, 2045, $\nu_{\text{C}=\text{C}}$ 2149; ^1H NMR (δ in CDCl_3) 0.13 (br s, Me_3Si). Polymer **3b** is hardly soluble in organic solvents, and therefore its ^{13}C and ^{29}Si NMR spectroscopic analysis could not be carried out.

TGA of the Polymers. On a platinum plate was placed ca. 5 mg of a polymer, and the plate was heated from 20 to 1000 °C at a rate of 20 °C/min under a nitrogen atmosphere. The results are summarized in Table 1.

Measurement of Conductivities of Polymer Films Doped with FeCl_3 and I_2 . A benzene solution of a polymer was cast as a thin film on a glass plate. After the solvent was evaporated, the film was dried in vacuo overnight and then held over FeCl_3 or I_2 powder in a glass vessel. Doping with FeCl_3 vapor was performed by heating the bottom of the glass vessel at 150 °C under reduced pressure (1 mmHg) for 15–42

h, while that with I₂ vapor was carried out at room temperature under atmospheric pressure. The conductivities of the polymers were determined by the four-probe method as listed in Table 1.

Preparation of Compound 4. A mixture of 270 mg (0.571 mmol) of **1a** and 415 mg (2.12 mmol) of Fe(CO)₅ in 5 mL of benzene was heated at 150 °C for 36 h in an autoclave. The solvent was evaporated, and the residue was chromatographed on silica gel using hexane as the eluent to give 294 mg (87% yield) of **4** as yellow crystals: mp 75–78 °C; MS *m/z* 612 (M⁺); UV (in THF; λ_{max}, nm (ε, M⁻¹ cm⁻¹)) 220 (ε = 43 900), 244 (ε = 32 200), 344 (sh, ε = 5100); IR (cm⁻¹) ν_{C=O} 1983, 2045, ν_{C=C} 2130; ¹H NMR (δ in CDCl₃) -0.19 (s, 3H, *exo*-MeSi), 0.17 (s, 18H, Me₃Si), 0.58 (s, 3H, *endo*-MeSi), 0.81–1.10 (m, 20H, EtSi); ¹³C NMR (δ in CDCl₃) 0.16 (*exo*-MeSi), 0.99 (Me₃Si), 4.70, 4.82, 8.48, 8.62 (EtSi), 9.23 (*endo*-MeSi), 54.23, 103.52 (C=C), 105.06, 115.76 (C≡C), 209.65 (CO); ²⁹Si NMR (δ in CDCl₃) -20.00, -0.65, 26.95. Anal. Calcd for C₂₇H₄₄O₃Si₅Fe: C, 52.91; H, 7.24. Found: C, 52.73; H, 7.17.

Preparation of Compound 6. A mixture of 73 mg (0.077 mmol) of **5** and 58 mg (0.30 mmol) of Fe(CO)₅ in 70 mL of benzene was irradiated with a high-pressure mercury lamp equipped with a Pyrex filter for 3 h. The solvent was evaporated, and the residue was chromatographed on silica gel using hexane as the eluent to give 50 mg (54% yield) of **6** (cis and trans, 1:1 mixture) as yellow solids: mp 75–78 °C; FAB-MS *m/z* 1226 (M⁺); UV λ_{max} (in THF; λ_{max}, nm (ε, M⁻¹ cm⁻¹)) 210 (ε = 74 600), 237 (ε = 55 000), 320 (ε = 15 400); IR (cm⁻¹) ν_{C=O} 1983, 2148, ν_{C=C} 2142; ¹H NMR (δ in CDCl₃) -0.19 (s, 6H, *exo*-MeSi), 0.14 (s, 36H, Me₃Si), 0.58 (s, 6H, *endo*-MeSi), 0.80–1.13 (m, 40H, EtSi); ¹³C NMR (δ in CDCl₃) 0.81, 0.87 (*exo*-MeSi), 0.96 (Me₃Si), 4.66, 4.75 (br.), 4.78, 8.02 (br.), 8.20, 8.30 (EtSi), 8.95 (*endo*-MeSi), 55.40, 95.78 (C=C), 98.82, 105.32, 105.36 (C≡C), 209.59 (CO); ²⁹Si NMR (δ in CDCl₃) -30.18, -30.09, -0.82, 27.34. Anal. Calcd for C₅₄H₈₈O₆Si₁₀Fe₂: C, 52.91; H, 7.24. Found: C, 52.79; H, 7.36.

X-ray Crystallographic Analysis of 4 and 5. All unique diffraction maxima with 0 < 2θ < 126.1° for **4** and 0 < 2θ < 125.7° for **5** were recorded on a Rigaku AFC-6C automated four-circle diffractometer using graphite-monochromated Cu Kα radiation (λ = 1.5418 Å). Refractions with I > 3σ(I) were used in the least-squares refinement. The structure was solved

by the SIR92 direct method¹⁴ and expanded using DIRDIF94 Fourier techniques.¹⁵ The non-hydrogen atoms were refined anisotropically. Neutral atom scattering factors were taken from Cromer and Waber.¹⁶ Anomalous dispersion effects were included in F_c¹⁷; the values for Δf' and Δf'' were those of Creagh and McAuley.¹⁸ The values for the mass attenuation coefficients are those of Creagh and Hubbel.¹⁹ All calculations were performed using the teXsan²⁰ crystallographic software package of Molecular Structure Corp.

MO Calculations. Ab initio MO calculations for compounds **8** and **9** were carried out with the Gaussian 94 program at the RHF/STO-3G level on a J932 server (CRAY) at the Information Processing Center, Hiroshima University. The molecular geometries were optimized by molecular mechanics (MM2).

Acknowledgment. We thank Sankyo Kasei Co. Ltd., Sumitomo Electric Industry, and Japan Chemical Innovation Institute for financial support.

Supporting Information Available: Figures giving ORTEP drawings with the full atomic numbering schemes and tables of atomic coordinates, anisotropic thermal parameters, and bond lengths and angles for compounds **4** and **5**. This material is available free of charge via the Internet at <http://pubs.acs.org>.

OM9805943

(14) Altomare, A.; Burla, M. C.; Camalli, M.; Cascarano, M.; Giacovazzo, C.; Guagliardi, A.; Polidori, G. *J. Appl. Crystallogr.* **1994**.

(15) Beurskens, P. T.; Admiraal, G.; Beurskens, G.; Bosman, W. P.; de Gelder, R.; Israel, R.; Smits, J. M. M. The DIRDIF-94 Program System; Technical Report of the Crystallography Laboratory; University of Nijmegen, Nijmegen, The Netherlands, 1994.

(16) Cromer, D. T.; Waber, J. T. In *International Tables for X-ray Crystallography*; Kynoch Press: Birmingham, England, 1974; Vol. IV, Table 2.2A.

(17) Ibers, J. A.; Hamilton, W. C. *Acta Crystallogr.* **1964**, *17*, 781.

(18) Creagh, D. C.; McAuley, W. J. In *International Tables for Crystallography*; Wilson, A. J. C., Ed.; Kluwer Academic: Boston, 1992; Vol. C, Table 4.2.6.8, pp 219–222.

(19) Creagh, D. C.; Hubbell, J. H. In *International Tables for Crystallography*; Wilson, A. J. C., Ed.; Kluwer Academic: Boston, 1992; Vol. C, Table 4.2.4.3, pp 200–206.

(20) teXsan: Crystal Structure Analysis Package; Molecular Structure Corp., The Woodlands, TX, 1985 & 1992.